FABRICATION AND ANTIBACTERIAL ACTIVITY OF ALLYL ISOTHIOCYANATE-LOADED CHITOSAN NANOPARTICLES FOR ENHANCED FOOD PRESERVATION

[1]Hoang-Anh CAO, [1]Jana PEKÁRKOVÁ, [2]Eliška BIRGUSOVÁ, [2]Lukáš RICHTERA

[1]Brno University of Technology, Central European Institute of Technology, Brno, Czech Republic, EU,
Hoang-Anh.Cao@ceitec.vutbr.cz, pekarkova@vut.cz

[2]Mendel University in Brno, Department of Chemistry and Biochemistry, Brno, Czech Republic, EU,
xbirguso@mendelu.cz, richtera@mendelu.cz

https://doi.org/10.37904/nanocon.2025.5009

Abstract

Allyl isothiocyanate (AITC) has been recognized for its potent antibacterial and antioxidant properties, positioning it as a promising agent for food preservation. However, its practical application in the food industry is significantly hindered by its high volatility and strong, unpleasant odor. To address these limitations, we utilized the multifunctional attributes of chitosan, a polysaccharide derived from chitin, to stabilize and enhance the efficacy of AITC. The abundance of amino and hydroxyl groups in chitosan chain facilitates strong interactions with AITC, thus achieving high encapsulation efficiency. Additionally, the inherent antibacterial property of chitosan synergizes with that of AITC, potentially reducing the required dose for effective microbial inhibition. In this study, AITC-loaded chitosan nanoparticles (AITC-CSNPs) were synthesized using a two-step emulsion-ionic gelation method. The characterization of the nanoparticles was performed using Dynamic Light Scattering (DLS) to determine their hydrodynamic size, zeta potential, and polydispersity index, while Scanning Electron Microscopy (SEM) provided detailed insights into their morphology and distribution. Afterwards, the antibacterial properties of AITC-CSNPs were evaluated on prevalent food-borne pathogens. The findings indicated that the as-synthesized AITC-CSNPs possessed a spherical shape with nanosize and demonstrated satisfactory antibacterial effects, thereby presenting a viable method for extending the shelf life of perishable food products.

Keywords: Allyl isothiocynate, chitosan nanoparticles, antibacterial properties, food preservation

1. INTRODUCTION

One of the primary challenges in food manufacturing is the control of pathogenic microorganisms during production. These pathogens contribute significantly to food spoilage, resulting in health problems, food waste, and economic losses [1]. In this context, allyl isothiocyanate (AITC), derived from plants of the Brassicaceae family, has garnered significant attention as a natural agent for food preservation [2-4]. AITC, a volatile sulfur-containing compound, contributes mainly to the strong flavors of mustard, wasabi, and horseradish [5]. Since the early 20th century, AITC has been noted for its potent antimicrobial [6] and antifungal [7] properties even at low concentrations. Since 2005, the U.S. The Food and Drug Administration (USFDA) designated AITC as Generally Recognized as Safe (GRAS) [8], while the European Food Safety Authority (EFSA) regulated its use as a food additive in the EU in 2010 [9]. Despite these advantages, the practical use of AITC in active food packaging is hindered by challenges related to its volatility, solubility, and controlled release over time [10]. In addition, its strong odor can negatively affect consumer acceptance [3]. To address these issues, encapsulation techniques have been developed to stabilize AITC for use in food processing. Recent studies have explored nanotechnology as a means of enhancing AITC's stability and efficacy of AITC. For example, Aytac et al. [11] demonstrated the incorporation of AITC-loaded β-cyclodextrin into electrospun nanofibers,

whereas Encinas-Basurto et al. [12] enhanced the functionality of AITC using poly(lactic-co-glycolic acid) nanocarriers.

In this study, chitosan (CS), a chitin-derived polysaccharide, was employed as a multifunctional biopolymer to entrap AITC. Firstly, CS exhibits remarkable characteristics, including non-toxicity, biocompatibility, and biodegradability, which are preferred for various applications including food preservation [13]. Secondly, CS possesses excellent antibacterial and antioxidant properties against a wide range of bacteria and fungi [14]. Furthermore, the abundance of amino and hydroxyl groups on the chain facilitates CS to interact with a plenty of active substances, thereby being promising to encapsulate productively AITC [15]. Indeed, Patil & Patel [16] described the successful fabrication of CS nanoparticles (CSNPs) loaded AITC with encapsulation efficiency of 88 % for breast cancer treatment. To the best of our knowledge, no study has demonstrated the synergistic antibacterial effect of CS and AITC in nanoformulations for food preservation.

Herein, this study aims to fabricate AITC-loaded chitosan nanoparticles (AITC-CSNPs) and explore their antibacterial properties. To achieve the research goal, the main objectives were specified as follows: (1) Synthesis of AITC-CSNPs using a two-step emulsion-ionic gelation method; (2) Characterization of AITC-CSNPs by Dynamic Light Scattering (DLS) and Scanning Electron Microscopy (SEM), and (3) Antibacterial assessment of AITC-CSNPs against common bacteria.

2. MATERIALS AND METHODS

2.1 Materials

Low molecular weight chitosan (CS) (50–190 kDa, 75–85 % degree of deacetylation), Sodium tripolyphosphate (TPP), Allyl isothiocyanate (AITC), Acetic acid, Tween 20 and all solvents were purchased from Sigma-Aldrich (Darmstadt, Germany) with quality of analytical grade. The following bacteria were provided by the Czech Collection of Microorganisms (Brno, Czech Republic): *S. aureus* (CCM 4223), Methicillin-resistant *S. aureus* (CCM 7110), and *E. coli* (CCM K12). Ultrapure water (18.2 MΩ·cm) was utilized in all steps of this study.

2.2 Preparation of unloaded and loaded-AITC Chitosan nanoparticles (CSNPs and AITC-CSNPs)

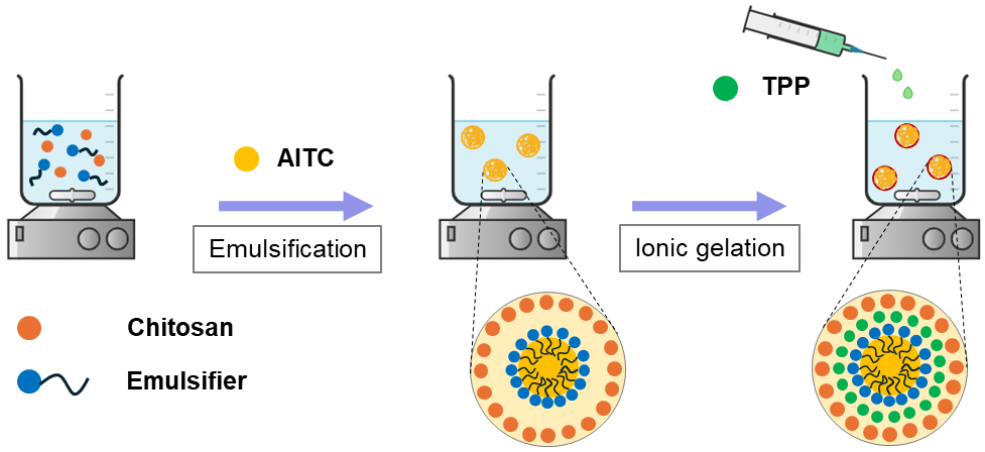

Figure 1 Scheme of encapsulation of Allyl isothiocyanate (AITC) in Chitosan nanoparticles (CSNPs)

The encapsulation of AITC in chitosan nanoparticles (AITC-CSNPs) was prepared in a two-step process (**Figure 1**) as reported by Patil and Patel [16]. In brief, 0.1 % CS solution (w/v) was stirred at 1000 rpm with 0.15 % Tween 20 and preheated to 50 °C. Then, AITC was added to achieve a ratio of CS:AITC by 1:0.5 w/w and emulsified under continuous stirring at 14000 rpm for 15 min at room temperature. Finally, a TPP aqueous solution of 0.1 % (w/v) was added using a microsyringe at 1 mL/min under continuous stirring to establish the

AITC-CSNPs. The mixture was kept for 1 hour under gentle stirring. The nanoparticles were collected by centrifugation and washed several times with ultrapure water. Afterwards, the AITC-CSNPs were stored at 4 °C for further analysis. The unloaded CSNPs were synthesized similarly as described above without presence of AITC. **Table 1** presents the detailed composition of CS, TPP, and AITC in each synthesis batch.

Table 1 Formulation of CSNPs and AITC-CSNPs

Code	AITC (mg/mL)	Ratio of CS:TPP (w/w)
F0 (CS:TPP 1:1)	0	1:1
F1 (CS:TPP 1:1)	0.5	1:1
F2 (CS:TPP 2:1)	0.5	2:1
F3 (CS:TPP 3:1)	0.5	3:1

2.3 Characterization of AITC-CSNPs

Dynamic light scattering (DLS)

The hydrodynamic size, polydispersity index (PDI), and zeta potential of CSNPs and AITC-CSNPs were provided by Dynamic light scattering (DLS) method using Zetasizer Nano ZS (Malvern Panalytical, UK) with the specifications as following: chitosan refractive index (RI) of 1.700, absorption index of 0.001 and water solvent RI of 1.33, with a viscosity of 0.8872 cP. All measurements were performed in triplicates.

Scanning Electron Microscopy (SEM)

SEM micrographs were obtained on Verios 460L (Thermo Fisher, USA) to explore morphology, shape and size of CSNPs and AITC-CSNPs. An accelerating voltage of 20 kV was applied at the working distance of 5 mm. Before imaging, all samples were coated with a 15-nm layer of gold using a coating device (EM ACE600, Leica, Germany) to achieve sufficient conductivity. The average particle size was estimated from at least 100 measurements using ImageJ from three SEM micrographs.

Determination of encapsulation efficiency (EE) of AITC-CSNPs

To evaluate the amount of encapsulated AITC, the supernatant was carefully separated from the AITC-CSNPs by centrifugation. A UV-Vis spectrophotometer was utilized to determine the absorbance of the supernatant at 248 nm. The quantity of AITC in the supernatant was calculated based on the calibration curve, which was constructed from the concentration of standard AITC solutions and their respective absorbances. As the initial amount of AITC added to the synthesis was defined, the encapsulation efficiency (EE) of AITC was calculated according to equation (1) as follows:

$$\text{EE}\ (\%) = \frac{\text{Initial AITC (mg)} - \text{AITC in supernatant (mg)}}{\text{Initial AITC (mg)}} \times 100\ \% \qquad (1)$$

2.4 Assessment of antimicrobial activity of AITC-CSNPs

The antimicrobial properties of CSNPs and AITC-CSNPs were assessed against common Gram-positive and Gram-negative bacteria, namely *S. aureus*, Methicillin-resistant *S. aureus*, and *E. coli.* Two commonly used methods, dics diffusion and broth microdilution, were employed in this study. For dics diffusion tests, filter paper discs were soaked in nanoformulation suspensions (10 mg/mL) and placed on bacterial inoculated Mueller-Hinton agar plates. The inhibition zones around the discs were measured after a 24-hour incubation period at 37 °C. In case of broth microdilution method, microbial suspensions (1.5×10^8 CFU/mL) were incubated with AITC, CSNPs, and AITC-CSNPs in concentration of 10 mg/mL to 0.156 mg/mL at 37 °C. The growth of bacteria were checked after 24h of the treatment.

3. RESULTS AND DISCUSSION

3.1 Hydrodynamic diameter and surface charge of AITC-CSNPs

Table 2 presents the hydrodynamic diameter and surface charge of the AITC-loaded and unloaded chitosan nanoparticle formulations. The size of the AITC-CSNP formulations ranged from 100.4 to 129.0 nm. The observed size reduction from formulations F1 to F3 correlated with the decreasing TPP amount, calculated as the mass ratio relative to that of chitosan. This trend aligns with the ionic crosslinking mechanism underlying the formation of the chitosan nanoparticles. The extent of this crosslinking network is primarily governed by the balance of negative charges from the amino groups on the chitosan chains and positive charges from the phosphate groups of TPP. Higher TPP concentrations promote a more extended crosslinking network, resulting in larger particle sizes. Additionally, a comparison between the unloaded (F0) and AITC-loaded (F1) formulations at the same CS/TPP ratio revealed that incorporating AITC increased particle size. This size increase was consistent with previous studies on the encapsulation of essential oils in chitosan nanoparticles [15]. The homogeneity of the nanoformulations was demonstrated by the polydispersity index (PDI). The nanoformulations in this study, with PDI values from 0.377 ± 0.010 to 0.571 ± 0.007 (**Table 2**), exhibited mid-range polydispersity. Zeta potential results of nanoformulations were in the range of +28.6 ± 0.9 mV to +36.4 ± 3.0 mV, which indicated a sufficient stability of them in aqueous solutions. Zeta potential values above +30 mV or below -30 mV are ideal, as they ensure adequate electrostatic repulsion, leading to a more stable suspension.

Table 2 Average hydrodynamic diameter, Polydispersity index (PDI), Zeta potential , Encapsulation efficiency (EE) of AITC loaded and unloaded CSNPs

Code	Average size (nm)	PDI	Zeta potential (mV)	EE (%)
F0	117.6 ± 1.2	0.377 ± 0.010	+28.9 ± 0.7	-
F1	129.0 ± 0.9	0.380 ± 0.008	+28.6 ± 0.9	7.08 ± 3.26 %
F2	124.4 ± 1.0	0.571 ± 0.007	+35.5 ± 0.7	4.32 ± 1.19 %
F3	100.4 ± 0.6	0.447 ± 0.012	+36.4 ± 3.0	1.87 ± 4.23 %

3.2 Encapsulation of AITC into Chitosan nanoparticles

In this study, UV spectrophotometry was utilized to evaluate the encapsulation efficiency of AITC in each formulation. The findings revealed promising results, with encapsulation values ranging from 1.87 % to 7.08 %. A clear trend emerged, showing that the encapsulation efficiency decreased as the TPP content in the nanoformulations was reduced. While the AITC-loaded chitosan nanoparticles (AITC-CSNPs) were small in size and exhibited good dispersion when prepared with lower TPP ratio, this advantage came at the cost of reduced encapsulation efficiency. This trade-off suggests that optimizing TPP levels is critical for balancing the particle size and encapsulation efficiency in the formulation process.

3.3 Morphology of AITC-CSNPs

SEM analysis was carried out to investigate the morphology and surface characteristics of the nanoformulations. The micrographs in **Figure 2** revealed nanoparticles with a spherical shape, which was typical for chitosan nanoparticles. The particle sizes for formulations F0 to F3, as determined by SEM, were 53.9 ± 7.5 nm, 54.1 ± 8.2 nm, 44.9 ± 6.8 nm, and 25.1 ± 2.1 nm, respectively. Although these values were smaller than those measured by DLS, the same trend in size was observed across the formulations. Specifically, the incorporation of AITC led to an increase in particle size (as seen in F0 and F1), whereas decreasing the proportion of TPP resulted in progressively smaller nanoparticles (as demonstrated in F1, F2, and F3). The difference in particle size obtained by DLS and SEM can be explained based on the particle aggregation phenomenon commonly encountered in polymeric nanoparticles. Unlike microscopy, the DLS

technique cannot determine the size of individual particles in aggregates, resulting in hydrodynamic diameters that can be up to 10 times larger than the dimensions of the particles determined by microscopy, such as TEM or SEM [17].

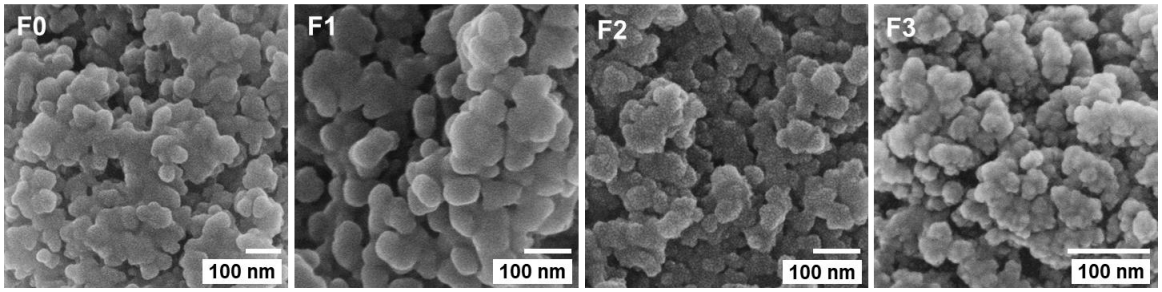

Figure 2 Representative SEM micrographs of CSNPs and AITC-CSNPs

3.4 Antimicrobial activity of AITC-CSNPs

Table 3 presents the minimum inhibitory concentrations (MIC) of AITC and nanoformulations against Gram-positive and Gram-negative bacteria. All formulations of AITC-CSNPs exhibited higher antimicrobial activity against *S. aureus* and Methicillin-resistant *S. aureus* than the free AITC and blank CSNPs. For *E. coli*, the lowest MIC was observed with nanoformulation F1, followed by higher values for free AITC and nanoformulations F2 and F3, respectively. Blank chitosan nanoparticles (CSNPs) showed no inhibitory effect on *E. coli* growth within the tested concentration range.

Table 3 Minimum inhibitory concentration (µg/mL) of AITC, CSNPs, and AITC-CSNPs against Gram-positive and Gram-negative bacteria

Microbial strains	AITC	F0	F1	F2	F3
S. aureus	625	1250	156.2	312.5	312.5
Methicillin-resistant *S. aureus*	1250	2500	312.5	625	625
E. coli	2500	>10,000	1250	5000	5000

The disc diffusion results showed limited inhibition in the growth of tested microorganisms. This outcome may be attributed to the limited diffusion of AITC and the nanoformulations into the agar medium.

4. CONCLUSION

In this study, AITC was successfully encapsulated in chitosan nanoparticles using a two-step ionic gelation technique, achieving a highest efficiency of 7.08 %. All nanoformulations exhibited characteristic spherical shapes, nanoscale sizes, and stability in aqueous media, as confirmed by the DLS and SEM results. Microbial assays demonstrated the enhanced antibacterial activity of AITC-loaded chitosan nanoparticles (AITC-CSNPs) against *S. aureus,* Methicillin-resistant *S. aureus,* and *E. coli*. The AITC-CSNPs showed higher efficacy compared with AITC or CSNPs alone at the same dosage, underscoring the synergistic effect of AITC integration within the CSNP matrix. However, further studies should be conducted to investigate the controlled release of AITC from these nanoformulations and to evaluate how the antibacterial efficacy varies with concentration and time.

ACKNOWLEDGEMENTS

This study was supported by the project CEITEC VUT-J-24-8615, Brno University of Technology and CzechNanoLab Research Infrastructure funded by MEYS CR (LM2023051)

REFERENCES

[1] AMIT, S.K., UDDIN, M.M., RAHMAN, R., ISLAM, S.M.R., KHAN, M.S. A review on mechanisms and commercial aspects of food preservation and processing. *Agriculture & Food Security*. 2017, vol. 6, no. 1, pp. 51.

[2] SHIN, J., HARTE, B., RYSER, E., SELKE, S. Active Packaging of Fresh Chicken Breast, with Allyl Isothiocyanate (AITC) in Combination with Modified Atmosphere Packaging (MAP) to Control the Growth of Pathogens. *Journal of Food Science*. 2010, vol. 75, no. 2, pp. M65-M71.

[3] KO, J.A., KIM, W.Y., PARK, H.J. Effects of microencapsulated Allyl isothiocyanate (AITC) on the extension of the shelf-life of Kimchi. *International Journal of Food Microbiology*. 2012, vol. 153, no. 1, pp. 92-98.

[4] KRAMER, B., WUNDERLICH, J., MURANYI, P. Impact of volatile allyl isothiocyanate on fresh produce. *Food Packaging and Shelf Life*. 2018, vol. 16, pp. 220-224.

[5] CORRALES, M., FERNÁNDEZ, A., HAN, J.H. *Innovations in Food Packaging (Second Edition)*. San Diego: Academic Press, 2014.

[6] LIN, C.-M., KIM, J., DU, W.-X., WEI, C.-I. Bactericidal Activity of Isothiocyanate against Pathogens on Fresh Produce†. *Journal of Food Protection*. 2000, vol. 63, no. 1, pp. 25-30.

[7] WINTHER, M., NIELSEN, P.V. Active Packaging of Cheese with Allyl Isothiocyanate, an Alternative to Modified Atmosphere Packaging. *Journal of Food Protection*. 2006, vol. 69, no. 10, pp. 2430-2435.

[8] USFDA. GRAS Claim notification for general Recognition of Safety of Allyl isothiocyanate in a food shelf-life extension and antio-sopilage system. GRN0180. 2005.

[9] EFSA. Scientific Opinion on the safety of allyl isothiocyanate for the proposed uses as a food additive. *EFSA Journal*. 2010, vol. 8, no. 12, pp. 1943.

[10] MOLLER, A., LEONE, C., KATARIA, J., SIDHU, G., RAMA, E.N., KROFT, B., THIPPAREDDI, H., SINGH, M. Effect of a carrageenan/chitosan coating with allyl isothiocyanate on microbial spoilage and quality of chicken breast. *Poultry Science*. 2023, vol. 102, no. 3, pp. 102442.

[11] AYTAC, Z., DOGAN, S.Y., TEKINAY, T., UYAR, T. Release and antibacterial activity of allyl isothiocyanate/β-cyclodextrin complex encapsulated in electrospun nanofibers. *Colloids and Surfaces B: Biointerfaces*. 2014, vol. 120, pp. 125-131.

[12] ENCINAS-BASURTO, D., IBARRA, J., JUAREZ, J., BURBOA, M.G., BARBOSA, S., TABOADA, P., TRONCOSO-ROJAS, R., VALDEZ, M.A. Poly(lactic-co-glycolic acid) nanoparticles for sustained release of allyl isothiocyanate: characterization, in vitro release and biological activity. *Journal of Microencapsulation*. 2017, vol. 34, no. 3, pp. 231-242.

[13] PRIYADARSHI, R., RHIM, J.-W. Chitosan-based biodegradable functional films for food packaging applications. *Innovative Food Science & Emerging Technologies*. 2020, vol. 62, pp. 102346.

[14] WANG, X., CHENG, F., WANG, X., FENG, T., XIA, S., ZHANG, X. Chitosan decoration improves the rapid and long-term antibacterial activities of cinnamaldehyde-loaded liposomes. *International Journal of Biological Macromolecules*. 2021, vol. 168, pp. 59-66.

[15] MONDÉJAR-LÓPEZ, M., CASTILLO, R., JIMÉNEZ, A.J.L., GÓMEZ-GÓMEZ, L., AHRAZEM, O., NIZA, E. Polysaccharide film containing cinnamaldehyde-chitosan nanoparticles, a new eco-packaging material effective in meat preservation. *Food Chemistry*. 2024, vol. 437, pp. 137710.

[16] PATIL, P.B., PATEL, J.K. Preparation, characterization, and in vitro cytotoxicity activity of allyl-isothiocyanate-embedded polymeric nanoparticles for potential breast cancer targeting. *Breast Cancer*. 2023, vol. 30, no. 6, pp. 1065-1078.

[17] FILIPPOV, S.K., KHUSNUTDINOV, R., MURMILIUK, A., INAM, W., ZAKHAROVA, L.Y., ZHANG, H., KHUTORYANSKIY, V.V. Dynamic light scattering and transmission electron microscopy in drug delivery: a roadmap for correct characterization of nanoparticles and interpretation of results. *Materials Horizons*. 2023, vol. 10, no. 12, pp. 5354-5370.